Numerical modeling and validation of hydrothermal liquefaction of a lignin particle for biocrude production

Jayathilake, Madhawa; Rudra, Souman; Rosendahl, Lasse A.

Published in:
Fuel

DOI (link to publication from Publisher):
10.1016/j.fuel.2021.121498

Publication date:
2021

Document Version
Publisher's PDF, also known as Version of record

Fuel 305 (2021) 121498

Contents lists available at ScienceDirect

Fuel

journal homepage: www.elsevier.com/locate/fuel

Full Length Article

Numerical modeling and validation of hydrothermal liquefaction of a lignin particle for biocrude production

Madhawa Jayathilake [a], Souman Rudra [a,*], Lasse A. Rosendahl [b]

[a] Department of Engineering Sciences, University of Agder, Jon Lilletuns vei 9, 4879 Grimstad, Norway
[b] Department of Energy Technology, Aalborg University, Pontoppidanstræde 101, 9220 Aalborg, Denmark

ARTICLE INFO

Keywords:
Lignin
Hydrothermal liquefaction
Numerical modelling
Shrinking-core
Oily film
Ash layer

ABSTRACT

Lignin liquefaction process under catalyst-free conditions in a temperature range from 573 K to 647 K is investigated with this mathematical model. Based on the theoretical understanding of the physical and chemical processes of the liquefaction process in subcritical temperatures, a comprehensive mathematical model for the decomposition of lignin by hydrolysis reaction pathway is developed on the results of a series of batch experiments. The model consists of four main sections. They are liquefaction of lignin particle, oily film, and inorganic (ash) layer formation behavior during the liquefaction, kinetic model to model further liquefaction process of initial products, and the layer model for the intraparticle processes. Hydrolysis of the lignin particle is modeled using the shrinking core concept. The formation of oily film and an inorganic layer around the lignin particle and their behavior is modeled considering water transport through layers, diffusion of products, and dissolution of products in water. Moreover, the layer model is used to obtain surface and center point temperatures of the particle using mass transfer. .The kinetic model consists of ten components and 21 reactions. . Variations of aromatic hydrocarbons and phenolic compounds are given significance. In the experimental study highest biocrude yield of 0.28 w/w_0 is obtained at an operating temperature of 573 K. Aromatic hydrocarbons are reduced from 0.23 w/w_0 to 0.145 w/w_0 with the increase of operating temperature from 573 K to 623 K. For an increase of operating temperature from 573 K to 623 K, phenol shows an increase from 2.5×10^{-4} w/w_0 to 3×10^{-3} w/w_0. At 573 K and with a particle of radius 0.08 mm, oily film and ash layer show a maximum thickness of 2×10^{-12} m and 7.5×10^{-3} m, respectively. Both oily film and ash layer show a faster formation and faster dissolution in water with increasing operating temperature. Finally, the model's liquefaction results are analyzed and validated with the experimental data and the literature data, where it shows a reasonable agreement.

1. Introduction

Lignin is the second most common earthbound biopolymer and the most significant naturally occurring source of aromatic compounds [1]. Lignin is a significant by-product of the paper and pulp industry [2]. The amount of lignin extracted in the western hemisphere's pulping process is estimated to be around 50 million tons per year [1]. Despite its relative abundance and colossal potential, lignin is still underutilized, partly due to its complex structure and difficulty breaking down. Lignin consists of three main phenylpropanoid monomers, and it is an irregular aromatic biopolymer[3]. The process of breaking down the complex structure is referred to as depolymerization. Depolymerization can be accomplished using different processes like thermochemical processes and enzymatic and catalytic cracking. The process temperatures range from 373 K to 1073 K. Depolymerization is performed in both sub and supercritical fluids [4,5].

Hydrothermal liquefaction (HTL), unlike other thermochemical processes, is usually done at moderate temperatures and shorter residence times at sub and supercritical conditions (T = 523 K – 647 K and P = 10 – 30 MPa) [6–8]. Four product streams can be obtained from a typical HTL conversion [9]. The bio-crude is considered the most desirable product among them as it can be further upgraded into various chemicals and liquid biofuels. Therefore, recent research on HTL has been centered on improving the yield and quality of bio-crude and bio-oil [10].

In recent years, some research has been reported on lignin's hydrothermal liquefaction to obtain different products [5,11–13]. In the hydrothermal liquefaction of lignin to produce phenolic compounds,

* Corresponding author.
E-mail addresses: rukshanj@uia.no (M. Jayathilake), souman.rudra@uia.no (S. Rudra), lar@et.aau.dk (L.A. Rosendahl).

https://doi.org/10.1016/j.fuel.2021.121498
Received 23 March 2021; Received in revised form 7 June 2021; Accepted 17 July 2021
Available online 26 July 2021

hydrolysis and cleavage of the ether bond and C–C bond, demethoxylation, alkylation, and condensation reactions occur, and these reactions seem to compete. Alternatively, the aromatic rings are not affected by hydrothermal reactions [14]. The lignin-derived phenolic compounds from the demethoxylation and alkylation will be intensified as the temperature increases. Therefore, due to the different functionalities of phenolic compounds, lignin offers the potential of producing many valuable chemicals [14].

In literature, different methods are used for modeling the liquefaction of lignin. Yong and Matsumara [15] studied lignin decomposition in subcritical conditions and proposed a detailed kinetic reaction scheme. Zhang et al. [16] proposed a two-phase decomposition scheme for kraft lignin liquefaction. Forchheim et al. [17] investigated the phenolic products from lignin hydrothermal depolymerization with a kinetic model. All these models are kinetic models which handled the liquefaction process. Besides, researchers have been using the shrinking core concept to model wood and cellulose liquefaction [18–20]. Further, few researches suggested a possible oily film formation during the liquefaction process of a biomass particle which raises the importance of modeling such an oily film [20,21].

Despite having much research and many models developed with only kinetic schemes, there is a void in modeling liquefaction as a complete process. Thus, it is scarce to find details on the shrinkage of the particle, mass transfer from the particle, and the temperature behavior inside the particle during the liquefaction process. Furthermore, the formation of oily film and ash layer is yet to be experimentally studied. Therefore, modeling the formation of the oily film and ash layer could clarify the liquefaction behavior and produce better explanations for particle decomposition behaviors at different process conditions. The model presented in this article consists of four main sections. They are liquefaction of lignin particle, oily film, ash layer formation behavior during the liquefaction, kinetic model to model further liquefaction process of initial products, and the layer model for the intraparticle processes. In the proposed model, several aspects such as transport of water to the surface of the particle, diffusion through the ash layer and oily film, adsorption on the particle surface, heterogeneous reaction, desorption of the products from the particle, diffusion of the products through the ash layer, and transport of products back to ambient through the dissolution of products in water are considered. With the layer model, the intraparticle process is modeled. Therefore, the particle's temperature behavior at the particle's surface and the mass transport from the particle to the system are investigated. Besides, the biocrude phase is important as it is considered a mix of six different chemicals (Aromatic hydrocarbons, guaiacol, catechol, phenol, o-cresol, and m-cresol). With this model, each chemical component's variation can be investigated. Therefore, this model gives a better insight into the lignin liquefaction.

2. Materials and method

2.1. Materials

The lignin feedstock is obtained from Sigma-Aldrich (CAS Number 8068–05-1). It is analyzed by performing both the proximate and ultimate analysis. The proximate analysis is performed with the use of a Nabertherm MORE THAN 30 – 3000 °C muffle furnace. The ultimate analysis is also performed for the feedstock using the PerkinElmer 2400 CHNS/O Series II elemental analyzer to determine its elemental composition. The analytical conditions in all the above cases are as follows: 1 g of feedstock is used for proximate analysis with the oven temperature at 378 K for 24 h to determine the moisture content and the muffle furnace temperature ranging from 523 K to 1173 K, respectively to determine the ash and volatile matter content. The feedstock sample weights used for the elemental analysis ranged from 0.9 mg to 1.5 mg and operated at room temperature. 1 g of the sample is used for the calorific test with oxygen as the combustion gas. Ultrapure water is used as the reaction solvent. During the calculations, all the components are normalized to 1 atom 'C' per molecule for simplification. The proximate and ultimate analysis results of the Alkali lignin are illustrated below, Table 1.Table 2.

2.2. Methods

In developing the model, the shrinking core model is developed and connected with the heterogeneous reactions to model the particle decomposition through hydrolysis. Afterwards, the formation of oily film and the inorganic (ash) layer is modeled. As the next step, the kinetic model is developed to model the further decomposition, polymerization, and rearrangement reactions. For the kinetic model, data is taken from the literature. As the next step, the layer model is developed and merged with the rest of the model to study the temperature behavior on the particle. Once the model is fully developed, model predictions are graphed along with laboratory's experimental data and data from the literature for validation. Fig. 1 shows a schematic diagram of the method used to develop the model.

2.2.1. Experimental procedure

The experimental study is carried out only to validate the results from the proposed model. Therefore, only the biocrude yields are quantified for validation purposes. The liquefaction experiment is performed in a steel tubular reactor from the HIP, with an internal volume of 24 ml. A feed slurry of 16 ml is fed into the reactor, with a feedstock/water ratio of 1:9 maintained for all experimental runs. Therefore, in each sample, 1.6 g of lignin is mixed with 14.4 ml of ultrapure water. A dead volume of 8 ml is maintained throughout all the runs. The reactor is sealed and purged with nitrogen to displace the air inside. The reactor is heated in a fluidized sand bath, suspended inside the sand bath with a shaft connected to the electric motor, for shaking the reactor during the test.

The reactor is heated until the reaction temperature is attained. Then the temperature is kept for residence times ranging between 10 and 20 mins. Same residence times are used for reaction temperatures between 573 K and 623 K at the sub-critical condition. At the end of each reaction, the reactor is taken out and put into the water at room temperature at once and kept for 30mins. The gaseous products are vented out and later calculated by mass balance. Acetone is used to extract the liquid and solid products, and the reactor is washed three times to ensure complete removal of the product. The collected solid (biochar) is washed further with acetone and water to ensure the complete removal of residual acetone and bio-crude. Then the char is oven-dried at 378 K for 24 h to quantify the biochar yield. The bio-crude and residual water content are separated from the acetone with a rotary evaporator by evaporating acetone at 335 K. Fig. 2 below shows the extraction process of each output from the liquefaction process.

All experimental tests are carried out under similar conditions and in quadruples to ensure repeatability of the results. According to Eq 1 below, the yields of biocrude and char obtained from the experimental study are calculated based on the lignin's carbon content.

$$\text{Product yield} = \frac{\text{Carbon available in product}}{\text{Initial Carbon available in the input lignin}} \quad (1)$$

Table 1
Proximate and Ultimate Analysis of Alkali lignin.

	Proximate Analysis (Wt%)			Ultimate Analysis (Wt%, d.b)			
	VM	ASH	FC	C	H	N	O
Current work	73	9.62	17.38	51.5	4.12	0.35	44.03
Literature [22]	72.60 (d.b)	9.50 (d.b)	17.90 (d.b)	49.0	4.4	0	(S & O) 46.6

VM = Volatile matter, FC = Fixed Carbon, d.b = dry base.

Table 2
Reaction type of each reaction used in the lignin liquefaction model.

Reaction type	Kinetic parameters
Hydrolysis	K_1, K_3, K_4, K_5
Dehydration	K_2
Polymerization	K_6, K_7, K_{16}
Decomposition	K_8 , K_{10} , K_{11} , K_{12} , K_{13} , K_{14} , K_{15} , K_{17} , K_{18} , K_{19} , K_{20} , K_{21}
Gasification	K_9
Rearrangement	K_{17}

The set of chemical reaction used for the kinetic model is presented in the supplementary document.

2.2.2. Method of modeling

2.2.2.1. Shrinking core approach and hydrolysis modeling. Frequently, model compounds are abundantly used for the kinetic models of hydrolysis studies [15,16,18,19,23–28]. The proposed model is influenced by a model developed for wood liquefaction and is a continuation of that work [18].

In the proposed model, lignin hydrolysis is modeled using a shrinking core system. The decomposition of the lignin particle is assumed to be only in the radial direction. Fig. 3 below shows a graphical model of the assumed shrinking core concept used for the proposed model [18].

The decomposition of the lignin particle creates an oily film around the particle surface. Besides, the ash produced by the decomposition of the particle forms a layer as well. Therefore, the approach of water monomers to the lignin particle as well as diffusion of biocrude produced in the initial hydrolysis reactions are affected. Therefore, this model discusses the formation, behavior, and impact of those two layers around the particle.

2.2.2.2. Decomposition of the lignin particle. The considered lignin particle system with a fully developed ash layer and the oily film is shown in Fig. 4. Hydrolysis of the lignin particle is determined by the developed reaction rate constant. The lignin particle's overall decomposition is a cumulative effect of each hydrolysis compound and occurs in the radial direction. The water monomer's diffusion through the aqueous film surrounding the lignin particle is modeled using water's mass transfer (when no oily film is present) from Kamio et al. [19]. The derivation of the decomposition of the lignin particle according to the shrinking core model is presented in section 1and from eq1 to eq 27 in the supplementary document.

Each chemical component's theoretical values are calculated using differential equations using the backward Euler method. From the differential equations, the variation of each chemical compound's concentrations is obtained in mol/m^3. Then, each chemical compound or resultant phase is presented as a percentage of the total input.

2.2.2.3. Layer model for intra-particle process modeling. In this paper, a layer model is implemented to study the intra-particle transport and subprocesses of the thermally thick lignin particle. Although the ash layer thickness and oily film thickness are small (10^{-7}mm and 10^{-12} mm, respectively), all the three layers present in the previous section are considered here. The lignin component is regarded as a single homogenous particle. The layer model is influenced by the work done by Mehrabian et al., 2012 [29]. Fig. 5 shows the layer model used in the proposed model.

The layer model treats the three layers in one dimension. This simplification is done to avoid model complexities. For the modeling purpose, it is assumed the particle boundary conditions are homogeneous, and all the points at a certain distance from the surface at a radial direction have the same conversion rates and temperatures [30].

As the conversion starts, the mass and thickness of the two layers in the particle are changed. Since the lignin particle started decomposing,

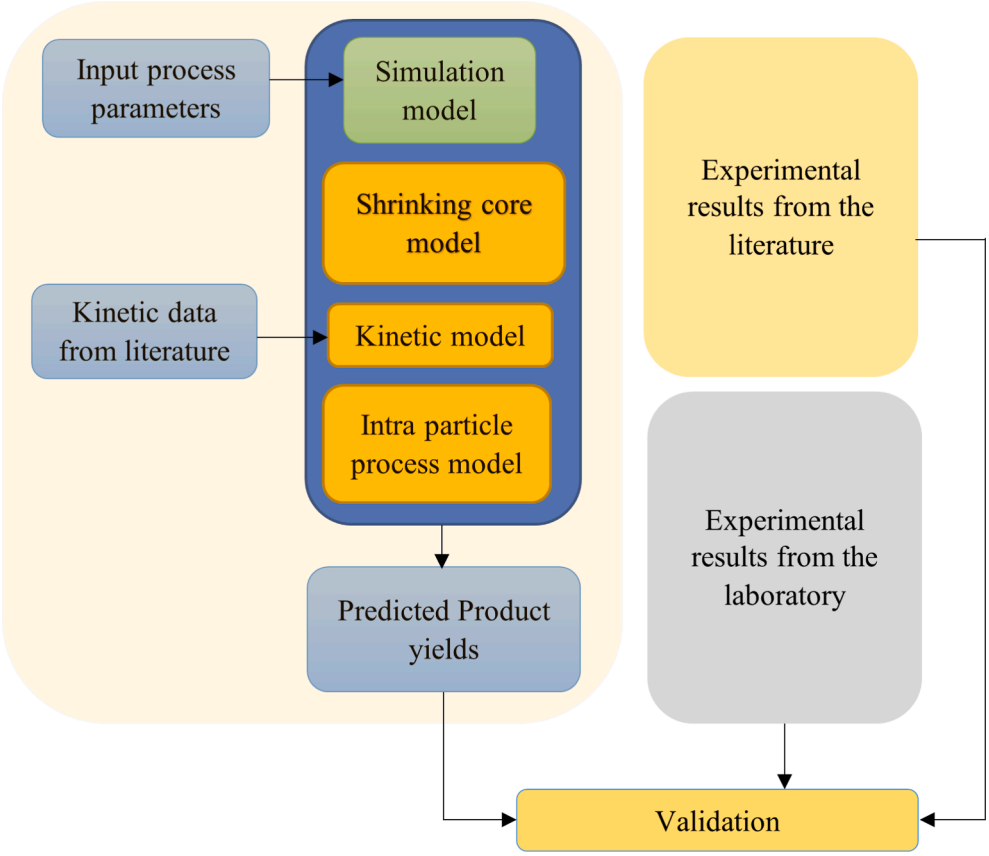

Fig. 1. Schematic diagram of the method used for developing the model.

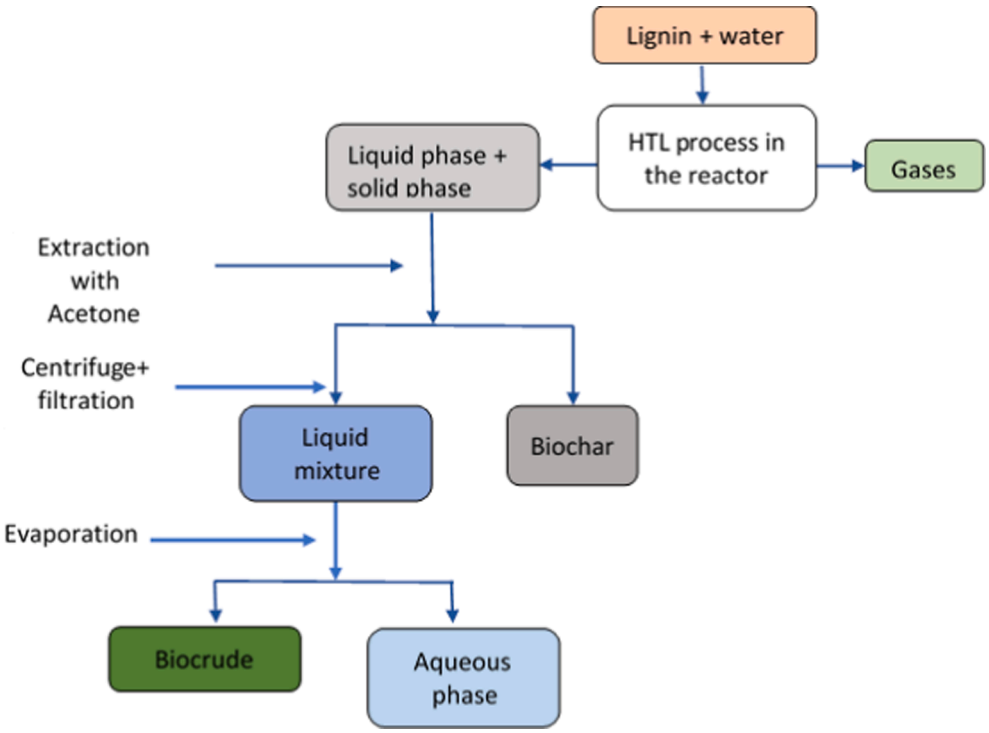

Fig. 2. Process Flow Diagram for the HTL experiment and separation techniques used.

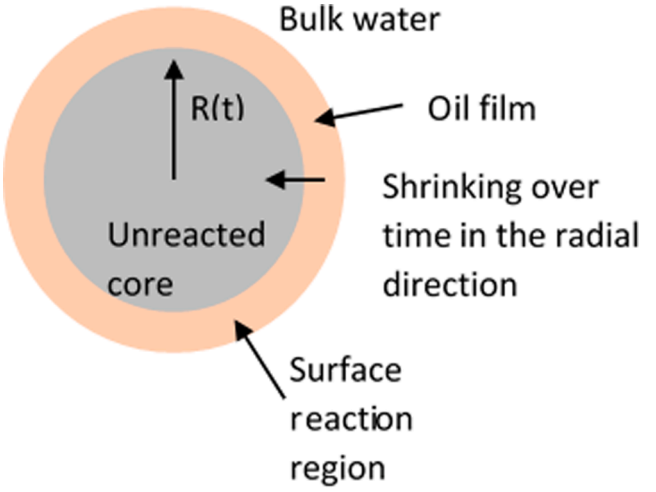

Fig. 3. Shrinking core model assumed for the hydrolysis of the lignin particle of model components submerged in water.

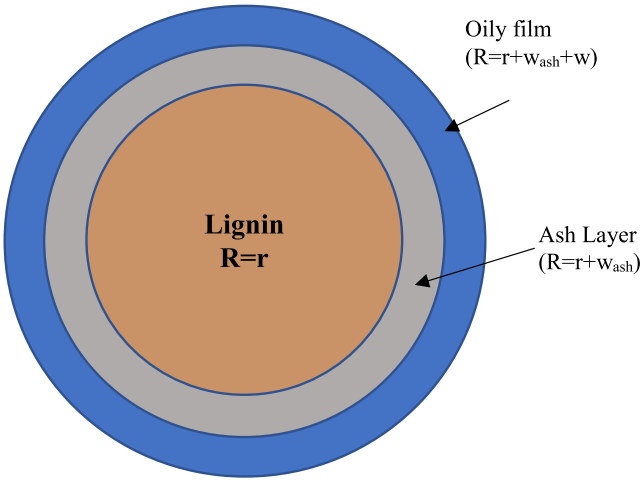

Fig. 4. Liginin particle system considered in the model.

the oily film will change its thickness according to the diffusion of water to the lignin particle surface, rate of hydrolysis, and dilution of the oily film in water. Along with this, the boundaries are moving towards the center of the particle as well. Therefore the density and the particle size may change during the thermal conversion of the particle.

The derivation of the equations related to the layer model is presented in section 2 and from eq 28 to eq 35 the supplementary document.

2.2.2.4. Kinetic model for lignin liquefaction. The lignin liquefaction model is a continuation of the previous work by the authors [18]. Fig. 6 shows the used reaction pathway of hydrolysis and the decomposition of lignin during the liquefaction process. For the lignin hydrolysis model, required kinetic parameters are taken from the literature [15–17,31,32]. In the supplementary document eq 36 to eq 46 in section 3 show the reactions incorporated in the lignin liquefaction model.

To acquire the results presented in this section, differential equations developed in the mathematical model are solved and discretized in MATLAB R2019b.

2.2.2.5. General assumptions and simplifications. The lignin particle is deemed as a spherical particle with a given radius. It is submerged in a vast water volume, which is much larger than the particle's radius. Hence the dilution of the hydrolysis products is assumed to be infinite at a given distance from the particle center. Moreover, it is assumed that there is always enough water to perform all the required hydrolysis reactions. The particle decomposition is assumed only in the radial direction. Some of the thermophysical properties are presumed to be constant throughout the process as well. (All the constant and temperature dependent thermophysical properties are mentioned in the Appendix) Particle is assumed to be homogenous in properties and

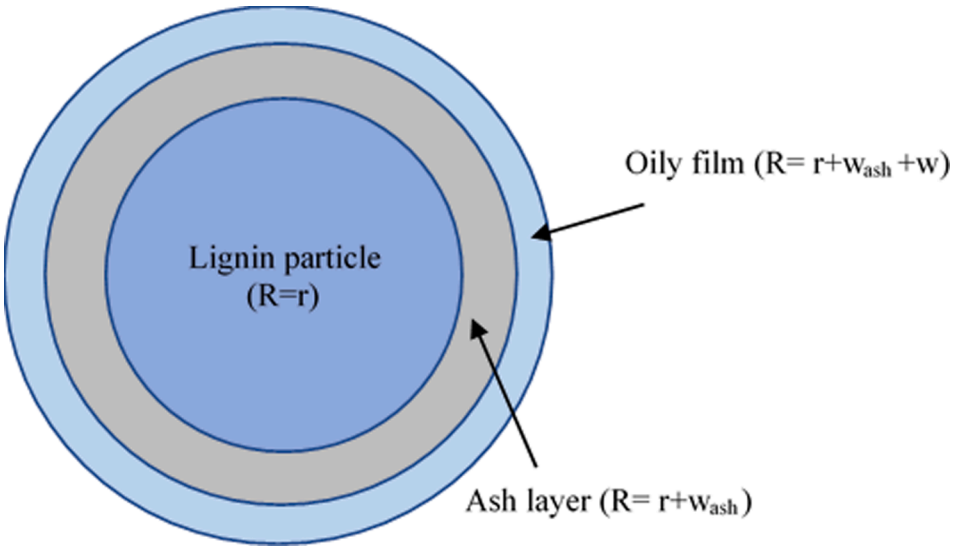

Fig. 5. Layer model considered for the intraparticle process.

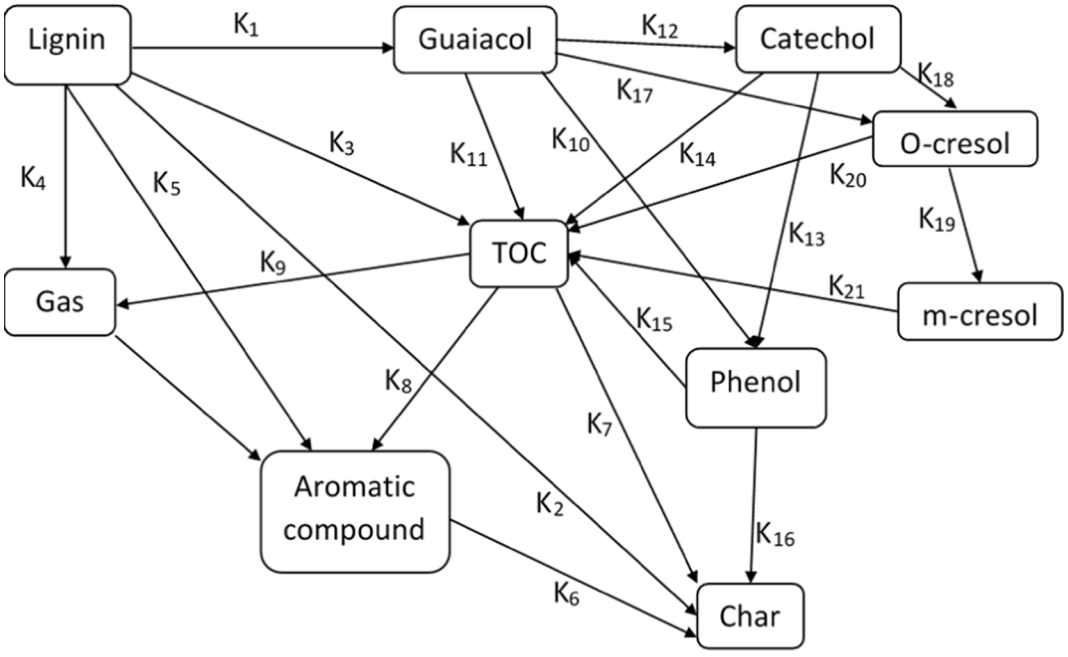

Fig. 6. Reaction pathways of lignin in hydrothermal conditions.

composition. Only ash is amassed around the particle, and then the oily film around the ash layer is assumed.

Hydrolysis reactions of lignin occur only on the surface of the particle at the given time. Nevertheless, for simplification, primary char is considered a direct degradation product of lignin and stays within the system and does not partake in any secondary reactions. Nevertheless, the composition of the particle is not changed with time or with the hydrolysis reaction. The particle decomposition is dependent only on the lignin left in the particle and the concentration of water at the particle surface. Lignin is partially soluble in water [33]. Besides in this model it is assumed that the whole lignin particle is available to react with water.

A simplified elemental balance is used for the model using an approximation for oxygen and hydrogen balance in the model compounds. Therefore, only Carbon balance is given importance due to the calculations' simplification. Only CO_2 is considered the main contributor to the gas phase.

Furthermore, due to the lack of literature, especially on the heating and fast reaction kinetics, some of the kinetic data is modified and fit to reaction equations to obtain the literature's yield values. It could be a possible reason for some of the over predictions and under predictions in the model. The layer model assumes that the oily film's outer surface has the same temperature as the surrounding water. The developed model calculations assumed no losses during the extraction process, which is a regular occurrence in an experimental procedure.

3. Results and discussion

3.1. Model predictions

In this section, different model predictions are demonstrated. First, the biocrude component variation with different variables is presented. Then oily film and ash layer behavior is illustrated and then followed by

the layer model predictions.

3.1.1. Biocrude component variation

Fig. 7 shows the impact of temperature variation on biocrude components. Temperature values of 573 K, 603 K, and 623 K are applied to examine the effect of temperature on the biocrude component yields. Generally lignin is hydrolyzed quickly and decomposes into various products [1,12,15,17]. According to Fig. 7, aromatic hydrocarbons, guaiacol, and m-cresol produce reduced yields with increased temperatures while phenol levels go up. Aromatic hydrocarbons represent benzene, toluene, and naphthalene, which are nonphenolic aromatic compounds. Higher yields of aromatic hydrocarbons at lower temperatures can be due to ionic reactions rather than free radical reactions [15].

Meanwhile, catechol yield decreases in yields with 603 K and then increases its yield with 623 K. A similar variation of catechol is observed

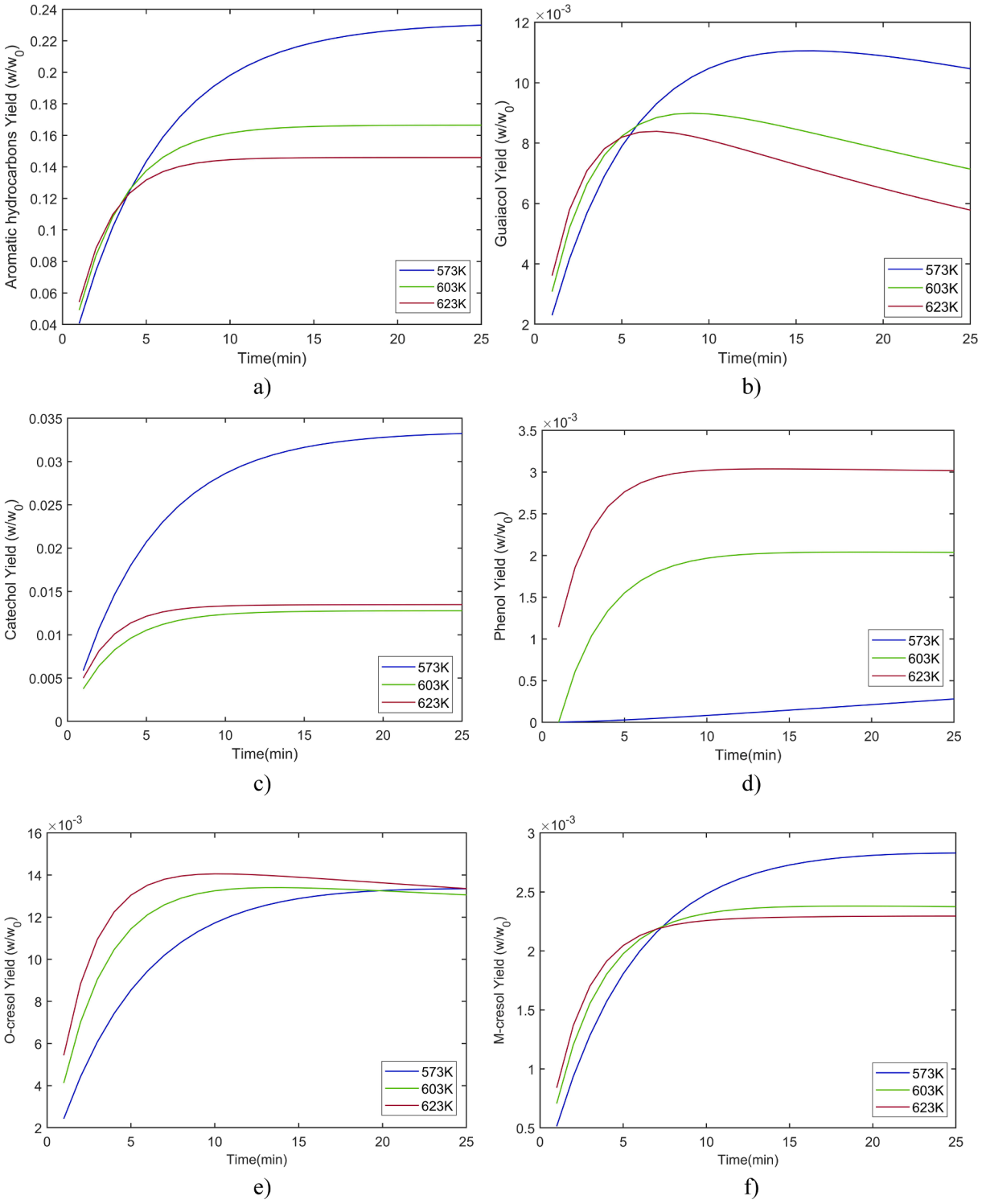

Fig. 7. Effect of temperature on production of components of biocrude at 573 K, 603 K and 623 K with a lignin particle radius of 0.08 mm a) Aromatic hydrocarbons b) Guaiacol c) Catechol d) Phenol e) O-cresol f) M-cresol.

by Yong and Matsumara [15] as well. Most of the components show a decrease in the yields with increasing temperature. The reason could be improved secondary reactions with a higher ionic water product and decomposition or repolymerization of these chemicals into char. Specially guaiacol is an intermedia degradation component in the lignin decomposition process [2]. With the increase of temperature and residence time, guaiacol decreases in the system, mainly due to its high reactivity and decomposition into catechol and phenols [32]. Since the bond energy of the aliphatic C −O bond is lesser than the aromatic C −O bond it is prone to be more reactive [15].

Moreover, the high ionic product and dielectric constant of water could impact the fast decomposition of guaiacol into phenol. Similar variation is shown by both guaiacol and catechol. Guaiacol is the main structure of softwood lignin. Catechol, o-cresol, and phenol are not

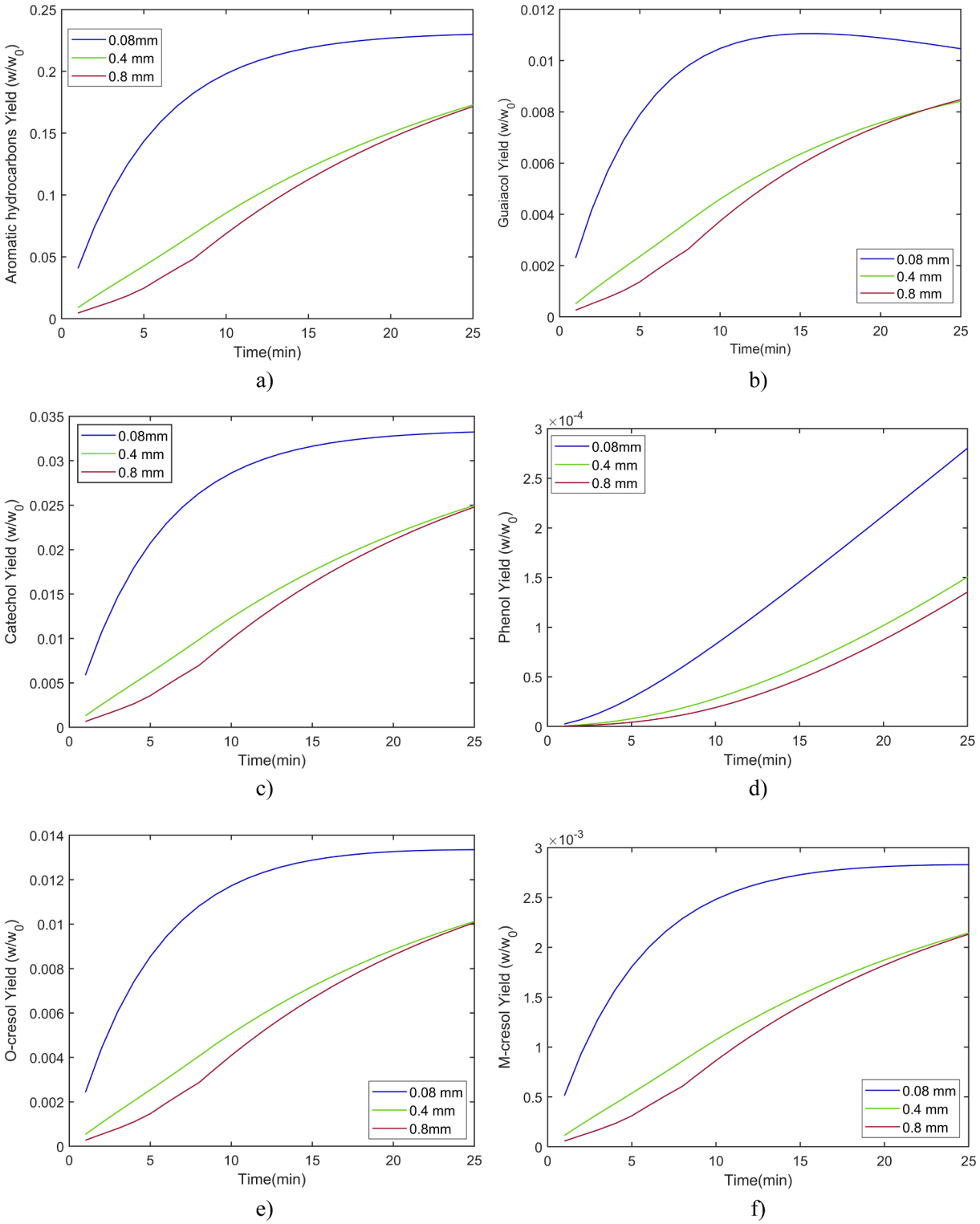

Fig. 8. Effect of particle size on the production of components of biocrude with lignin particle radius of 0.08 mm, 0.4 mm, and 0.8 mm at 573 K a) Aromatic hydrocarbons b) Guaiacol c) Catechol d) Phenol e) O-cresol f) M-cresol.

present in natural lignin and are only produced by the secondary decomposition or hydrolysis of guaiacol [2,15,34–36]. Therefore, the variation of catechol, o-cresol, and phenol is heavily impacted by guaiacol in the system. Similar behavior of phenol and guaiacol is observed by Pińkowska et al. 2012, [17,32]. In addition, Forchheim et al. 2014 reported that the catechol, phenols, and stable intermediates are produced through the reactive intermediates, which is similar to guaiacol in this study [16]. M-cresol is a direct derivate from o-cresol where m-cresol is possibly created through alkyl rearrangement [34].

According to Fig. 7, with all the considered chemicals except guaiacol, yields tend to stay approximately constant with longer residence times for all the considered temperatures. Understandably, guaiacol shows a decrease with the longer residence time where it shows a maximum of $11 \times 10^{-3} w/w_0$ at 15 min residence time. With this observation, it can be determined that any factor resulting in a higher yield of monomers such as temperature (553 K-643 K) or longer residence times helps both repolymerization and depolymerisation [3]. Therefore, for guaiacol and catechol to decrease and phenol to increase simultaneously, can be supported. The phenol's behavior with temperatures can be justified by the observations from Forchheim et al. 2014 [16].

The particle size diminution reasoning is to have a better specific area of biomass to the liquefaction medium. Nonetheless, access to the fine particles can be difficult at times, and the behavior of the yields with bigger particles can be of interest. However, as, change of particle radius makes a low impact on yields, subcritical water is a proper heat transfer medium [37]. For this study, three different particle radii sizes (0.08 mm, 0.4 mm, and 0.8 mm) are used. Fig. 8 shows the variation of biocrude component variation with different particle radius.

Fig. 9 below shows the decomposition of lignin particles with different particle radius. With a bigger particle radius, lignin shows a reduced decomposition rate. Therefore, with Fig. 9, the above fact of reduced production of biocrude components with increasing radius is supported by observing the lignin's slower decomposition.

Three different heating rates (1 K/min, 3 K/min, and 5 K/min) are applied to the model to analyze the heating rate's impact on the biocrude components. Fig. 10 below shows the yield variation of the products with different heating rates in a temperature range of 573 K to 640 K.

With 1 K/min heating rate, is used the particle stay longer at lower temperatures and thus the reactions can also occur at these lower temperatures. However, this behavior does not mean that the lignin particle has faster decomposition. Besides, a decomposition at lower temperatures due to the longer residence time at these temperatures. According to Fig. 10, Lignin does not significantly change yields with the heating rate variation. Except for the phenol production, other biocrude component yields are not significantly changed by the heating rate. Besides, at 640 K, phenol production is reduced to $3 \times 10^{-4} w/w_0$ from $1.75 \times 10^{-3} w/w_0$ when the heating rate is grown from 1 K/min to 5 K/min. Ultimately when the temperature value reaches 640 K (the critical point is at 647 K), product yields have become more stable except for guaiacol and phenol. This can be mainly due to the further decomposition of guaiacol to phenol. Nevertheless, the impact of the heating rate at short residence times is evident. Therefore, the impact of heating rates on both the initial kinetics of lignin decomposition and decomposition of guaiacol can be observed from these results. This brings out the importance of the heating rate on the fast liquefaction concept. Akhtar and Amin, 2011 [37] hinted at the reasoning behind higher char yields with higher heating rates due to the secondary reactions' dominance. Eq 38, Eq 39, and Eq 46 in supplementary document showcase those reactions where higher heating rates promote higher char yields instead of producing biocrude. In a previous work by the authors and Akhtar and Amin, 2011 [37], this fact is supported by illustrating the increase of char yield and a decrease of biocrude yield with the higher heating rate.

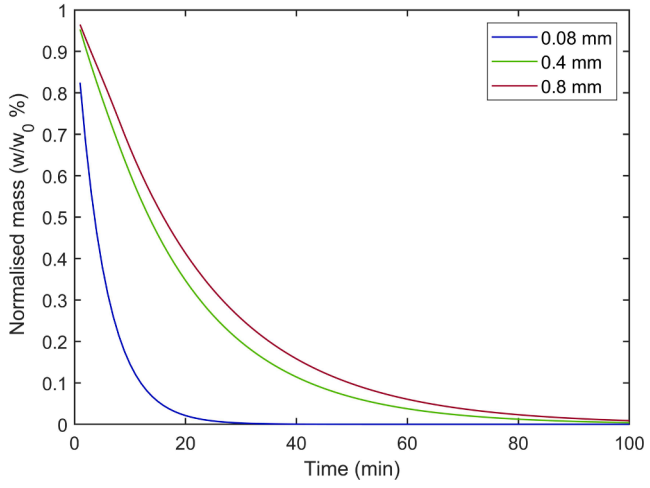

Fig. 9. Lignin decomposition with different particle radius of 0.08 mm, 0.4 mm and 0.8 mm at 573 K.

3.1.2. *Oily film and ash layer behavior*

The behavior of oily film and the ash layer with different operating temperatures is shown in below Fig. 11. According to Fig. 11, the oily film and ash layer have the maximum thicknesses after the reactions are started. This can be due to the initial fast decomposition of lignin. As soon as the particle is submerged in the water, no oily film or ash layer exists. Therefore, there is no resistance for water to reach the lignin particle surface. Nevertheless, with the reactions progress, the oily film and ash layer are formed, and the water monomer's movement to the particle surface is impeded. As time increases, both the oily film and ash layer come to equilibrium and dissolve into the system.

However, according to Fig. 11, oily film thickness increases dramatically with higher operating temperatures while it dissolves quickly. The rapid increase of the oily film can be justified by the initial rapid growth of aromatic hydrocarbons with higher temperatures. In another way, the oily film's behavior might have an impact on the product yields too. Similarly, with the ash layer, the initial rapid increase could be due to the fast initial hydrolysis of lignin under unobstructed water monomer arrival to the particle surface. Both the oily film and the ash layer are relatively thinner with lower temperatures, which helps both water and the products quickly diffuse through them. More water is gone through to the lignin particle surface, which allows hydrolysis to happen.

Moreover, thinner oily film and ash layer could allow guaiacol to quickly come out to the water to complete the secondary decomposition and produce more secondary products. With higher operating temperatures, due to the rapid increase of the oily film and the ash layer, water diffusion is hampered, leading to reduced lignin's initial hydrolysis. Potentially, this could have an impact on reduced yields of biocrude at higher operating temperatures. Therefore a further study of the formation of oily film and the ash layer can be significant. Dissolution of the ash layer is dependent on the oily film thickness as well.

According to Fig. 11b and Fig. 12b, the ash layer's thickness is much higher than the oily film. Therefore, ash layer formation might have a more significant impact on the liquefaction.

Below, Fig. 12 shows the oily film's behavior and the ash layer with different heating rates. Oily film and the ash layer show a thicker formation with higher heating rates. When the biocrude phase behavior is compared with this, it might create hints on the possible impact of oily film and ash layer thicknesses on the biocrude components' yields. Thicker oily film and ash layers could obstruct water monomers' arrival to the particle surface and the diffusion of guaiacol to the water medium.

When a particle radius is of the power of 10^{-5} m is utilized, the oily film thickness and ash layer thickness are of the power of 10^{-12} m and 10^{-7} m, respectively. Hence, there might not be a significant impact of

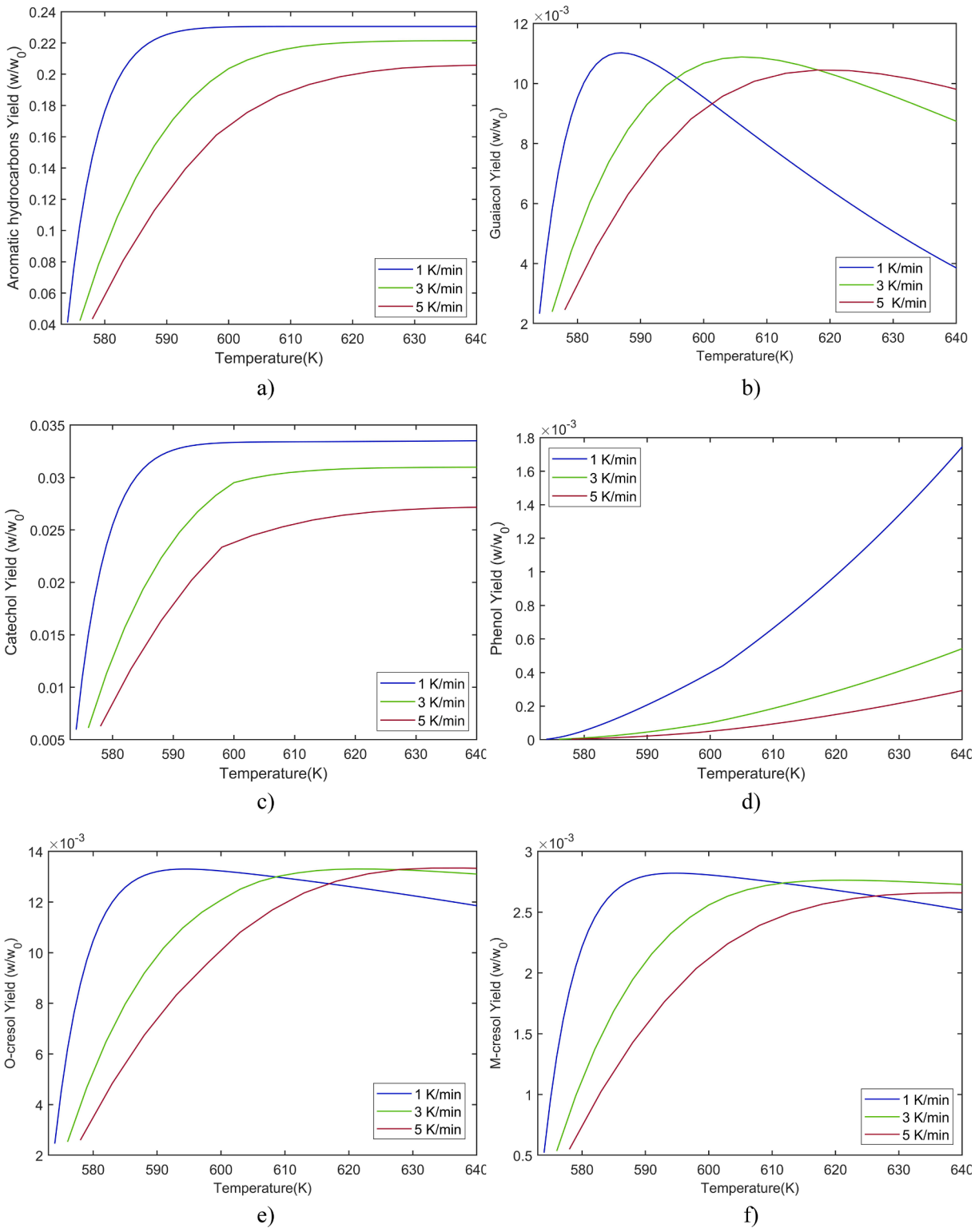

Fig. 10. Effect of heating rate on production of components of biocrude with a lignin particle radius of 0.08 mm a) Aromatic hydrocarbons b) Guaiacol c) Catechol d) Phenol e) O-cresol f) M-cresol.

oily film and ash layer thickness on the liquefaction. Therefore, the actual impact of the thickness of the oily film and ash layer is yet to be tested experimentally. Furthermore, benzene is used as the model compound for the oily film, and the actual dissolution properties of essential chemicals present in biocrude can be much different from the values used here. Likewise, the properties used for ash are taken from lignin ash. Besides, ash's actual behavior and dissolution properties in the liquefaction conditions can differ from those used for the model. Moreover, these aspects are difficult to study experimentally. Therefore, the oily film and ash layer's actual dissolution properties can be much different from what is observed here.

3.1.3. *Intraparticle behavior during liquefaction*

Fig. 13 shows the particle center temperature and particle surface

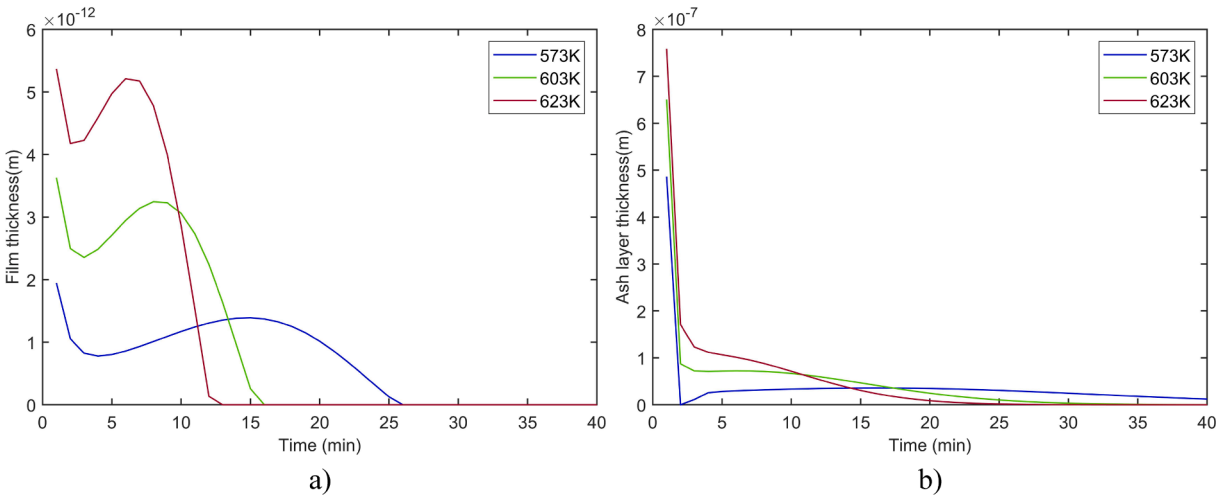

Fig. 11. Impact of temperature on oily film and ash layer formation with a lignin particle radius of 0.08 mm at 573 K, 603 K, and 623 K a) Oily film b) Ash layer.

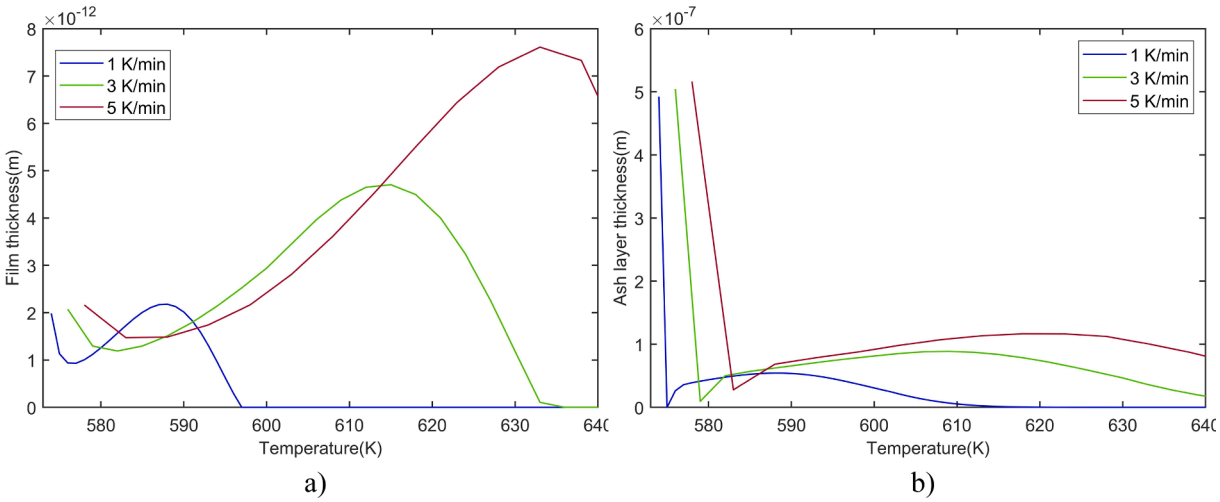

Fig. 12. Impact of heating rate on oily film and ash layer formation with heating rates of 1 K/min, 3 K/min and 5 K/min with a lignin particle radius of 0.08 mm a) Oily film b) Ash layer.

temperature during the liquefaction process. A slower thermal conductivity or an increase of ash layer thickness could lead to higher resistance against the heat transfer, and as a result, a decrease in the particle center temperature is visible. As shown in Fig. 14, the lignin mass loss is consistent. The water monomer diffusion rate primarily controls the hydrolysis rate. With lignin mass is lost with hydrolysis, the available surface area decreases due to the decreasing particle radius. The reduction of surface area could lead to reduced mass transfer. However, the particle temperature increases gradually.

Once the lignin is wholly consumed, the ash layer should be cooled rapidly towards the water phase temperature. Nevertheless, simultaneously the ash layer dissolves in the water too. In theory, due to particle heat-up and endothermic evaporation, the particle's temperature should be slightly lower than the surrounding temperature at the beginning. It is also assumed that the particle surface gets to the surrounding water temperature at once.

When volatile components start to release, the exothermic reactions around the particle increase the surface temperature. The slight rise in the surface temperatures from the surrounding water temperature in Fig. 13 explains it. Therefore during hydrolysis, the particle surface temperature increases and heats the gas phase by convective heat transfer.

The layer model calculates the mass and energy sources that are used in the species governing equations. The considered species calculations obtain few factors which are applied as boundary conditions for the layer model. These parameters are temperature, species concentrations, and available water concentration at each boundary. Furthermore, the species concentrations and the temperature around the particle are time-dependent and directly affected by the species generated by the lignin conversion through the hydrolysis process.

Model predictions show a slight increase in the particle center temperature and the surface during the hydrolysis process. The reason could be an exothermic reaction during the hydrolysis and decomposition of lignin [2], creating new stable bonds than in the lignin structure. Moreover, the further repolymerization of exothermic reactions at the particle surface could cause an increased particle surface temperature.

Subsequently, the hydrolysis rate of lignin, which is exponentially dependent on temperature, is responsible for the particle mass loss rate. Moreover, the empirical constants and data for the hydrolysis rate are obtained under certain process conditions. Therefore, any changes in these conditions might impact the validity of the hydrolysis rates, mass loss, and the calculated temperature values.

This model assumes that the char formed from the dehydration (Eq 37 in the supplementary document) stays within the particle without taking part in the reactions. Therefore, even when the lignin is completely hydrolyzed, the model particle is still available. Hence the

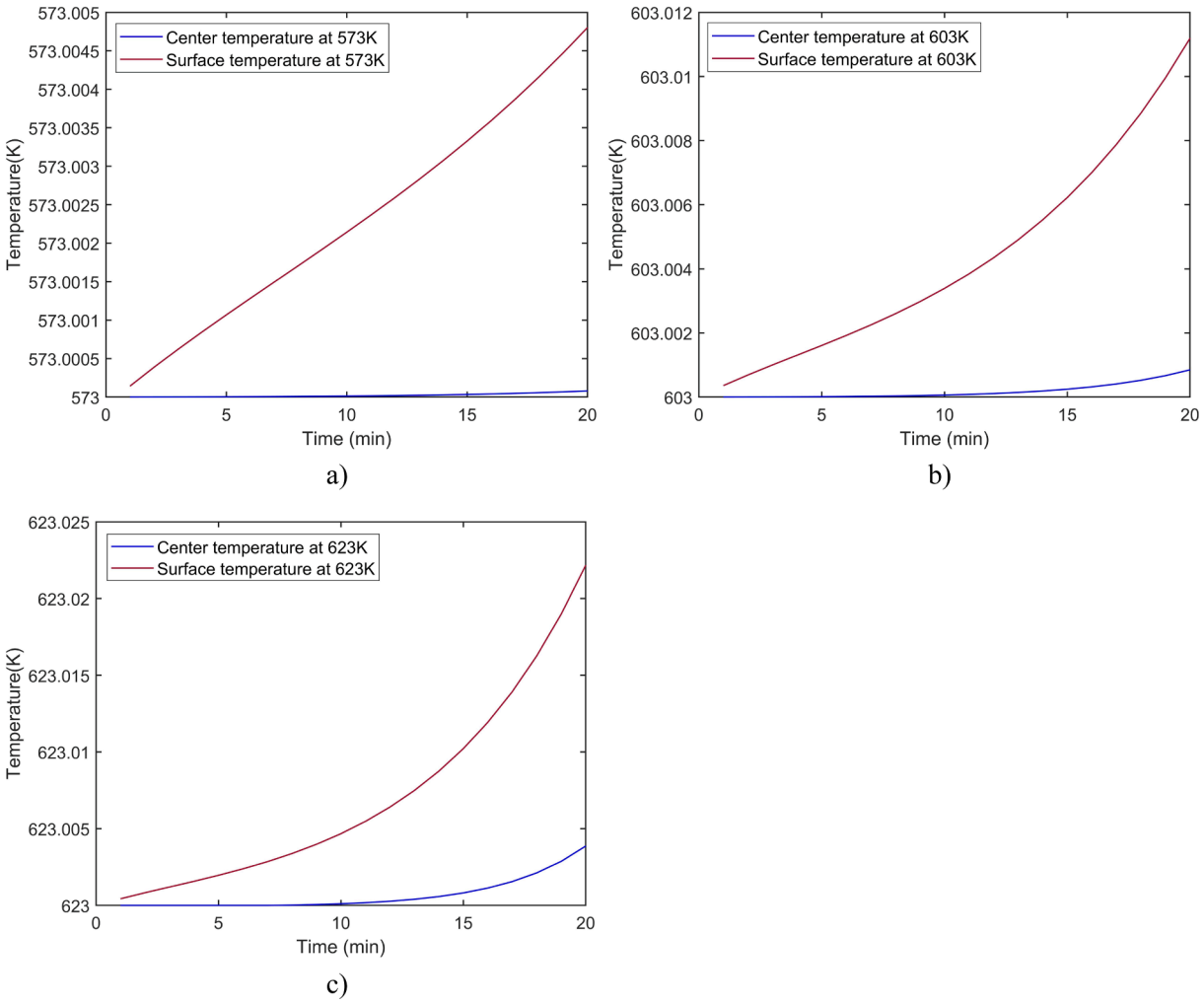

Fig. 13. Particle temperature profiles at different temperatures with a lignin particle radius of 0.08 mm a) 573 K, b) 603 K, c) 623 K.

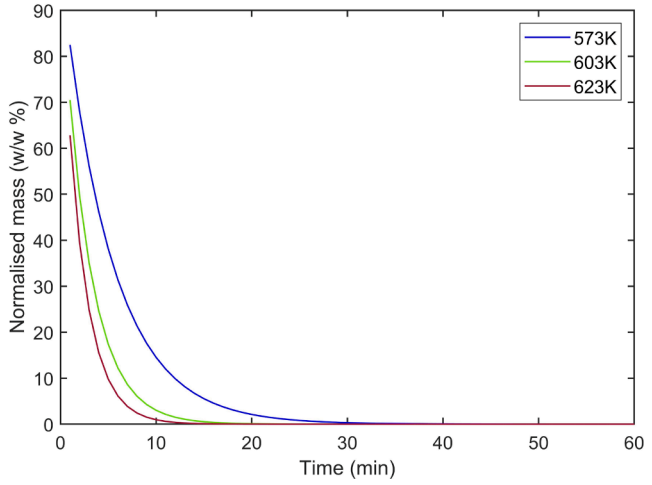

Fig. 14. Normalized mass profile at different temperatures of 573 K, 603 K, and 623 K with a lignin particle radius of 0.08 mm.

particle center temperature is kept calculating, and it does not show any difference after the total hydrolysis of lignin. That explains the model still has space to improve in the future.

Although the lignin layer disappears, due to the non-reactive char availability inside the ash layer, the model senses a particle's availability. Therefore, until the ash layer is fully dissolved, the particle consists of char and behaves as a regular lignin particle and shows the same effect on the temperature variation.

The particle mass predicted by the model decreases faster with higher temperatures (Fig. 14) and slower heating rates (Fig. 15a). These values are calculated solely on the empirical constants and developed differential equations. Due to the unavailability of experimental data on these parameters, it is difficult to determine whether these predictions are correct. Nevertheless, according to Fig. 15b, the particle surface temperature starts going down after coming to a maximum value with different heating rates. The reason can be the full dissolution of the ash layer after the complete hydrolysis of lignin. When the ash layer is fully dissolved, char that remained inside the ash layer released into the system. Then the particle does not exist anymore.

3.2. Validation

Validation of this model is done in two steps. First, the model's overall biocrude yield predictions are validated using the experimental study data from the lab-scale HTL reactor at the University of Agder, Norway. For the experiments, 573 K, 603 K, and 623 K temperatures are considered, and the yield values are reported below in Fig. 16.

According to the experimental data and model predictions, when the operating temperature increased, it has reduced the biocrude yield. This could be due to the promotion of the repolymerization reactions, which would yield more char in the secondary reactions [15,32]. Moreover,

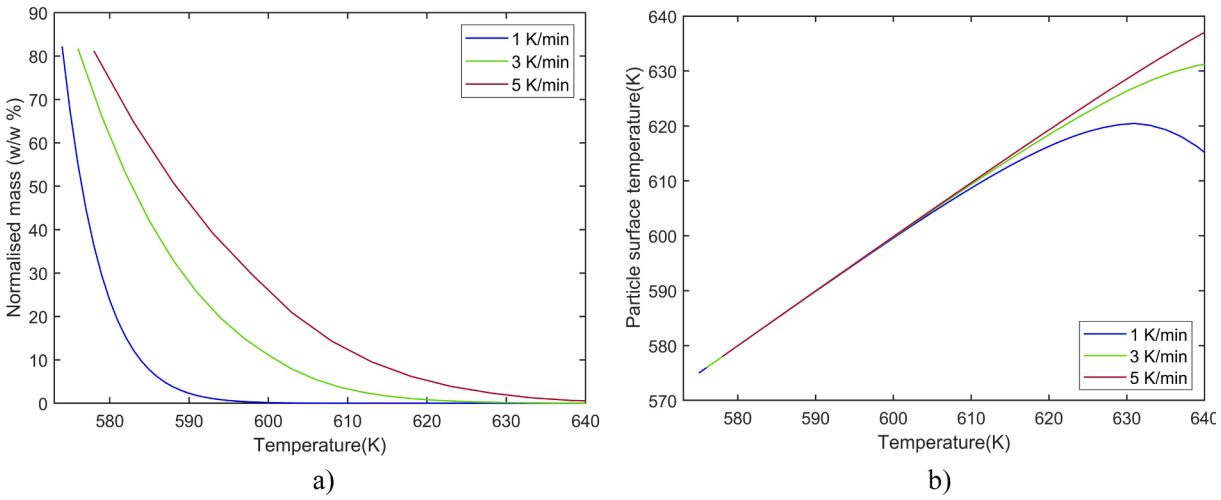

Fig. 15. Normalized mass profiles and particle surface temperature at different heating rates with heating rates of 1 K/min, 3 K/min and 5 K/min with a lignin particle radius of 0.08 mm a) Normalized mass profile b) Particle surface temperature.

when the operating temperature increases and goes close to the critical point, the process goes towards hydrothermal gasification, where it produces more gas [15,17]. According to Ye et al. 2012 [31], increased operating temperature and residence time promote further decomposition of lignin where it helps further repolymerization. This could ultimately result in overall biocrude yield reduction [15,32].

The second validation step is done using the experimental data, kinetic data, and process conditions used by Yong and Matsumara [15]. In this step, the main components of the biocrude phase considered in this work are validated. Therefore, the kinetic data and the process conditions from Yong and Matsumara [15] are used as inputs for the model, and predictions from the model are graphed along with the experimental values and model predictions obtained in their work. The validation plots are shown in Fig. 17. In their work, 603 K is not considered as an experimental operating temperature. Therefore, 603 K is not considered for the validation plots.

Ever Since the particle size of the lignin used by Yong and Matsumara [15] is not reported, a general radius size of 80 μm is used for the lignin particle. Different concentrations, loading conditions, different reaction routes, and kinetics could affect yield values. In most of the validation plots model predicted data shows a deviation from the initial experimental data, taken below two seconds residence time. This could be due to the unavailability of precise initial kinetic data to feed the model.

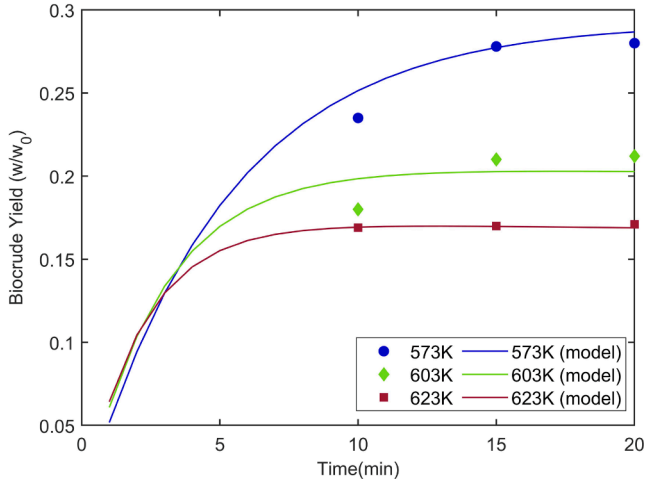

Fig. 16. Lignin Liquefaction model validation Biocrude at 573 K, 603 K and 623 K.

Besides, in the proposed model, the particle decomposition mechanism is given attention. Therefore, the temperature variation in the particle, oily film, and ash layer behavior and the mass transfer from the particle impact the deviations from the experimental results. Furthermore, during the modeling process only benzene is used as the model compound for the oily film. Properties of ash used for the model might not be the same as the liquefaction conditions. Thus, these factors can be vital in matching the experimental results exactly. Nevertheless, With the increase of residence time, the model data shows an excellent agreement with the experimental data.

4. Conclusion

The model is validated using lignin, experimental liquefaction data obtained at the University of Agder, and literature. The predictions of the model agree with the literature showing reliability.

At 573 K with a particle size of 0.08 mm, aromatic hydrocarbons show the maximum yield of 0.23 w/w_0. Slower heating rates have produced better yields with all the chemical components. For longer residence times and close to the critical point, heating rates reduce the yields. Oily film and ash layer shows a similar formation process and similar behavior at different process conditions.

Some of the model input values can differ from actual liquefaction conditions and could change the actual results. Since the availability of data used for this model is limited and bears a high uncertainty in the yields due to the different workup processes, it is better not to obtain results in a quantitative sense. The behavior of the oily film and ash layer is not experimentally tested. Therefore more experimental studies are required to validate some of the results obtained. In this article, only subcritical temperatures are considered. When the temperatures are shifted to the supercritical region, the ionic product of water, as well as the kinetic parameters change dramatically. Therefore, modeling the same scenarios in supercritical conditions needs a separate study.

CRediT authorship contribution statement

Madhawa Jayathilake: . **:** Conceptualization, Methodology, Software, Data curation, Writing - original draft, Investigation. **Souman Rudra:** Supervision, Writing - review & editing. **Lasse A. Rosendahl:** Supervision.

Declaration of Competing Interest

The authors declare that they have no known competing financial

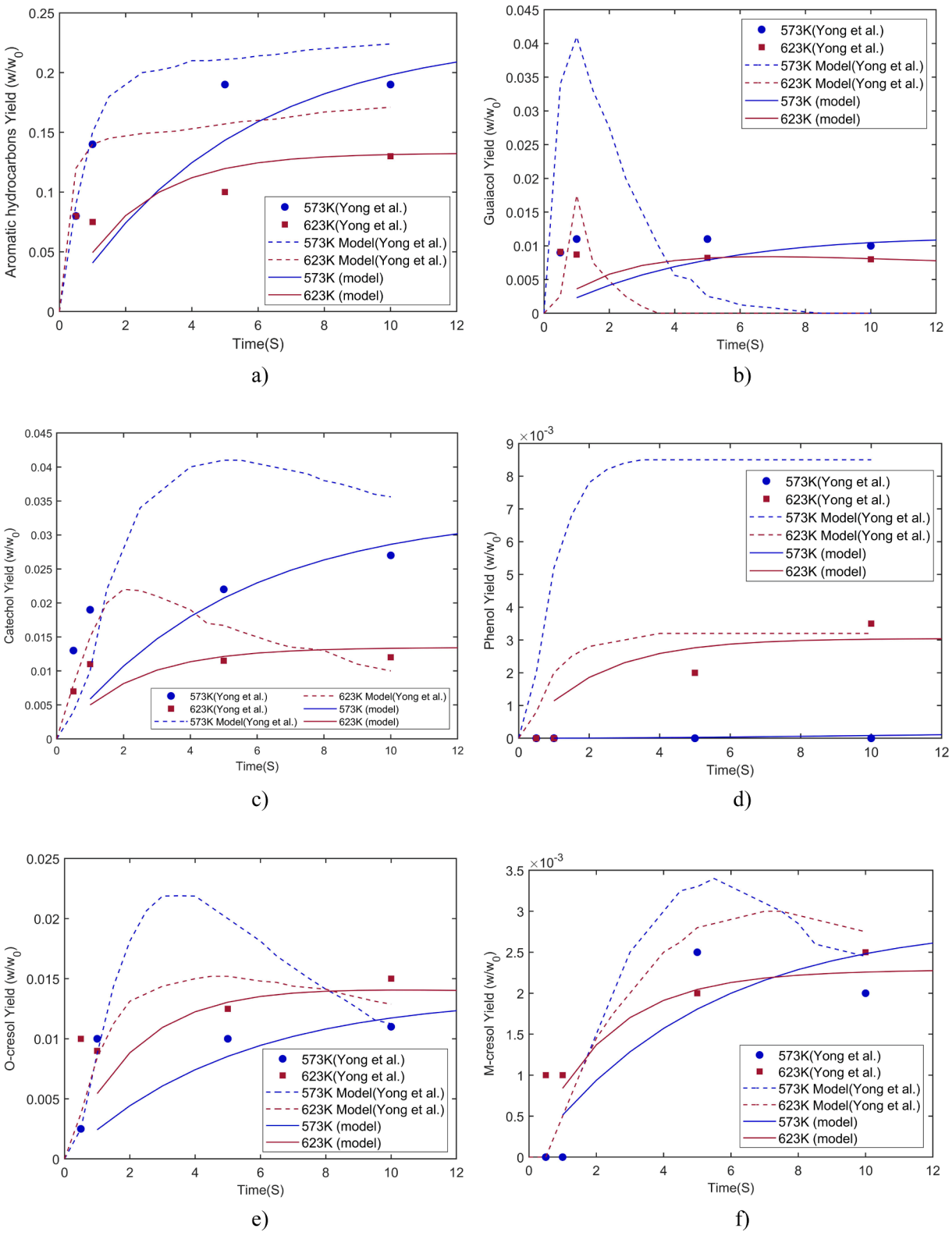

Fig. 17. Biocrude phase validation a) Aromatic hydrocarbons b) Guaiacol c) Catechol d) Phenol e) O-cresol f) M-cresol.

interests or personal relationships that could have appeared to influence the work reported in this paper.

Acknowledgment

This study was conducted as part of the Ph.D. research at the Department of Engineering Sciences, funded by the Faculty of Engineering and Science, University of Agder.

Appendix A. Supplementary data

Supplementary data to this article can be found online at https://doi.

org/10.1016/j.fuel.2021.121498.

References

[1] Arturi KR, Strandgaard M, Nielsen RP, Søgaard EG, Maschietti M. Hydrothermal liquefaction of lignin in near-critical water in a new batch reactor: influence of phenol and temperature. J Supercrit Fluids 2017;123:28–39. https://doi.org/10.1016/j.supflu.2016.12.015.

[2] Brebu M, Vasile C. Thermal degradation of lignin – a review. Cellul. Chem. Technol. 2010;44(9):353–63.

[3] Kozliak EI, Kubátová A, Artemyeva AA, Nagel E, Zhang C, Rajappagowda RB, et al. Thermal liquefaction of lignin to aromatics: efficiency, selectivity, and product analysis. ACS Sustain Chem Eng 2016;4(10):5106–22. https://doi.org/10.1021/acssuschemeng.6b01046.

[4] Becker J, Wittmann C. A field of dreams: lignin valorization into chemicals, materials, fuels, and health-care products. Biotechnol Adv 2019;37(6):107360. https://doi.org/10.1016/j.biotechadv.2019.02.016.

[5] Fache M, Boutevin B, Caillol S. Vanillin production from lignin and its use as a renewable chemical. ACS Sustain Chem Eng 2016;4(1):35–46. https://doi.org/10.1021/acssuschemeng.5b01344.

[6] Elliott DC, Biller P, Ross AB, Schmidt AJ, Jones SB. Hydrothermal liquefaction of biomass: Developments from batch to continuous process. Bioresour Technol 2015;178:147–56. https://doi.org/10.1016/j.biortech.2014.09.132.

[7] Castello D, Pedersen TH, Rosendahl LA. Continuous hydrothermal liquefaction of biomass: a critical review. Energies 2018;11(11). https://doi.org/10.3390/en11113165.

[8] Rudra S, Jayathilake M, "Hydrothermal Liquefaction of Biomass for Biofuel Production," in Reference Module in Earth Systems and Environmental Sciences, Elsevier, 2021. doi: 10.1016/B978-0-12-819727-1.00043-1.

[9] de Caprariis B, De Filippis P, Petrullo A, Scarsella M. Hydrothermal liquefaction of biomass: Influence of temperature and biomass composition on the bio-oil production. Fuel Nov. 2017;208:618–25. https://doi.org/10.1016/j.fuel.2017.07.054.

[10] Yang J, He Q (Sophia), Corscadden K, Niu H, Lin J, Astatkie T, "Advanced models for the prediction of product yield in hydrothermal liquefaction via a mixture design of biomass model components coupled with process variables," Appl Energy, 233–234, 2019, 906–915. doi: 10.1016/j.apenergy.2018.10.035.

[11] Lui MY, Chan B, Yuen AKL, Masters AF, Montoya A, Maschmeyer T. Unravelling some of the key transformations in the hydrothermal liquefaction of lignin. ChemSusChem 2017;10(10):2140–4. https://doi.org/10.1002/cssc.201700528.

[12] Sauer J, Dahmen N, Hornung U, Schuler J, Kruse A. Hydrothermal liquefaction of lignin. J Biomater Nanobiotechnol 2017;8(1):720–6. https://doi.org/10.4236/jbnb.2017.81007.

[13] Kang S, Li X, Fan J, Chang J. Classified separation of lignin hydrothermal liquefied products. Ind Eng Chem Res 2011;50(19):11288–96. https://doi.org/10.1021/ie2011356.

[14] Kang S, Li X, Fan J, Chang J. Hydrothermal conversion of lignin: a review. Renew Sustain Energy Rev 2013;27:546–58.

[15] Yong T-L-K, Matsumura Y. Kinetic analysis of lignin hydrothermal conversion in sub- and supercritical water. Ind Eng Chem Res 2013;52(16):5626–39. https://doi.org/10.1021/ie400600x.

[16] Zhang B, Huang H-J, Ramaswamy S. Reaction kinetics of the hydrothermal treatment of lignin. Appl Biochem Biotechnol 2008;147(1–3):119–31. https://doi.org/10.1007/s12010-007-8070-6.

[17] Forchheim D, Hornung U, Kruse A, Sutter T. Kinetic modelling of hydrothermal lignin depolymerisation. Waste Biomass Valorization 2014;5(6):985–94. https://doi.org/10.1007/s12649-014-9307-6.

[18] Jayathilake M, Rudra S, Rosendahl LA. Hydrothermal liquefaction of wood using a modified multistage shrinking-core model. Fuel 2020;280:118616. https://doi.org/10.1016/j.fuel.2020.118616.

[19] Kamio E, Sato H, Takahashi S, Noda H, Fukuhara C, Okamura T. Liquefaction kinetics of cellulose treated by hot compressed water under variable temperature conditions. J Mater Sci 2008;43(7):2179–88. https://doi.org/10.1007/s10853-007-2043-6.

[20] Mosteiro-Romero M, Vogel F, Wokaun A. Liquefaction of wood in hot compressed water Part 2–Modeling of particle dissolution. Chem Eng Sci 2014;109:220–35. https://doi.org/10.1016/j.ces.2013.12.039.

[21] Vogel F, Catalytic Conversion of High-Moisture Biomass to Synthetic Natural Gas in Supercritical Water, in Handbook of Green Chemistry, American Cancer Society, 2010, pp. 281–324. doi: 10.1002/9783527628698.hgc024.

[22] ShuNa C, Wilks C, ZhongShun Y, Leitch M, ChunBao X. Hydrothermal degradation of alkali lignin to bio-phenolic compounds in sub/supercritical ethanol and water-ethanol co-solvent. Polym Degrad Stab 2012;97(6):839–48.

[23] Kamio E, Takahashi S, Noda H, Fukuhara C, Okamura T. Effect of heating rate on liquefaction of cellulose by hot compressed water. Chem Eng J 2008;137(2):328–38. https://doi.org/10.1016/j.cej.2007.05.007.

[24] Pińkowska H, Wolak P, Złocińska A. Hydrothermal decomposition of xylan as a model substance for plant biomass waste – hydrothermolysis in subcritical water. Biomass Bioenergy 2011;35(9):3902–12. https://doi.org/10.1016/j.biombioe.2011.06.015.

[25] Pronyk C, Mazza G. Kinetic modeling of hemicellulose hydrolysis from triticale straw in a pressurized low polarity water flow-through reactor. Ind Eng Chem Res 2010;49(14):6367–75. https://doi.org/10.1021/ie1003625.

[26] Shoji D, Kuramochi N, Yui K, Uchida H, Itatani K, Koda S. Visualized kinetic aspects of a wood block in sub- and supercritical water oxidation. Ind Eng Chem Res 2006;45(17):5885–90. https://doi.org/10.1021/ie0604775.

[27] Shoji D, Sugimoto K, Uchida H, Itatani K, Fujie M, Koda S. Visualized Kinetic Aspects of Decomposition of a Wood Block in Sub- and Supercritical Water. Ind Eng Chem Res 2005;44(9):2975–81. https://doi.org/10.1021/ie040263s.

[28] Yong T-L-K, Matsumura Y. Reaction kinetics of the lignin conversion in supercritical water. Ind Eng Chem Res 2012;51(37):11975–88. https://doi.org/10.1021/ie300921d.

[29] Mehrabian R, Zahirovic S, Scharler R, Obernberger I, Kleditzsch S, Wirtz S, et al. A CFD model for thermal conversion of thermally thick biomass particles. Fuel Process Technol 2012;95:96–108. https://doi.org/10.1016/j.fuproc.2011.11.021.

[30] Thunman H, Leckner B, Niklasson F, Johnsson F. Combustion of wood particles—a particle model for eulerian calculations. Combust Flame 2002;129(1):30–46. https://doi.org/10.1016/S0010-2180(01)00371-6.

[31] Ye Y, Zhang Y, Fan J, Chang J. Novel method for production of phenolics by combining lignin extraction with lignin depolymerization in aqueous ethanol. Ind Eng Chem Res 2012;51(1):103–10. https://doi.org/10.1021/ie202118d.

[32] Pińkowska H, Wolak P, Złocińska A. Hydrothermal decomposition of alkali lignin in sub- and supercritical water. Chem Eng J 2012;187:410–4. https://doi.org/10.1016/j.cej.2012.01.092.

[33] Jayathilake M, Rudra S, Akhtar N, Christy AA. Characterization and evaluation of hydrothermal liquefaction char from alkali lignin in subcritical temperatures. Materials 2021;14(11). https://doi.org/10.3390/ma14113024.

[34] Wahyudiono, Sasaki M, Goto M. Thermal decomposition of guaiacol in sub- and supercritical water and its kinetic analysis. J Mater Cycles Waste Manag 2011;13(1):68–79. https://doi.org/10.1007/s10163-010-0309-6.

[35] Kleinert M, Barth T. Phenols from lignin. Chem Eng Technol 2008;31(5):736–45. https://doi.org/10.1002/ceat.v31:510.1002/ceat.200800073.

[36] Lawson JR, Klein MT. Influence of water on guaiacol pyrolysis. Ind Eng Chem Fundam 1985;24(2):203–8. https://doi.org/10.1021/i100018a012.

[37] Akhtar J, Amin NAS. A review on process conditions for optimum bio-oil yield in hydrothermal liquefaction of biomass. Renew Sustain Energy Rev 2011;15(3):1615–24. https://doi.org/10.1016/j.rser.2010.11.054.